applied sciences

MDPI

Article

# Theoretical Prediction and Safety Evaluation of Adjacent Pipeline Deformation Caused by Connecting Channel Excavation Reinforced with Freezing Method

**Jun Zhang [1,2,*], Jiguo Liu [1,2], Shuoren Fu [3] and Zequn Hong [3]**

[1] CCCC Second Highway Consultant Co., Ltd., Wuhan 430056, China; liujiguo@ccccltd.cn
[2] Research and Development Center on Tunnel and Underground Space Technology, CCCC, Wuhan 430056, China
[3] School of Mechanics and Civil Engineering, China University of Mining and Technology, Xuzhou 221116, China; ts22030036a31@cumt.edu.cn (S.F.); zqhong@cumt.edu.cn (Z.H.)
* Correspondence: zhangjun98@ccccltd.cn

**Abstract:** Underground excavation by freezing method can ensure the safety of the surrounding structures. The influence of excavation of a connecting channel between two tunnels by freezing method on adjacent pipelines is studied in this paper. Combined with field measurement, numerical simulation, and theoretical analysis, the stress and deformation law of the whole process of channel excavation by freezing method is studied. Based on Euler–Bernoulli beam theory prediction, the influence of temperature field and excavation parameters on the longitudinal deformation of pipeline is analyzed. The results show that the excavation rate significantly affects the pipeline settlement, and the settlement surges when the excavation rate exceeds 1.0 m/d. At the same time, the thick frozen soil wall formed by low freezing temperatures enhances the supporting ability and effectively reduces the formation disturbance and settlement. The study focuses on the influence of connecting channel excavation on the pipelines under uniform formation conditions, and puts forward the evaluation method of pipeline safety to provide a theoretical reference for engineering practice.

**Keywords:** freezing method; connecting channel; theoretical prediction; safety evaluation

check for updates

**Citation:** Zhang, J.; Liu, J.; Fu, S.; Hong, Z. Theoretical Prediction and Safety Evaluation of Adjacent Pipeline Deformation Caused by Connecting Channel Excavation Reinforced with Freezing Method. *Appl. Sci.* **2024**, *14*, 9274. https://doi.org/10.3390/app14209274

Academic Editor: Ricardo Castedo

Received: 28 August 2024
Revised: 27 September 2024
Accepted: 1 October 2024
Published: 11 October 2024



## 1. Introduction

With the acceleration of urbanization, the development and utilization of underground space are becoming more and more extensive, and the construction of subway tunnels and their affiliated communication channels has become an important part of urban infrastructure [1,2]. However, in the construction process of tunnels and communication channels, especially when freezing technology is used for geotechnical reinforcement [3,4], its impact on the existing upper buildings has become a key problem to be solved urgently. Although freezing technology can effectively control the groundwater flow and enhance the formation stability, the temperature field change caused by it, the frost-heaving effect of soil, and the deformation in the subsequent thawing process may cause adverse effects on the upper buildings, such as foundation settlement and structural cracking [5,6]. Therefore, it is of great significance to deeply study the influence law of freezing of contact channels on the existing upper buildings to ensure the construction safety of underground engineering and protect the structural stability of existing buildings [7,8].

In the research field of tunnel–soil–building interaction, scholars at home and abroad have carried out a lot of work, especially on the influence of tunnel construction on underground pipelines, and have made remarkable progress [9,10]. These research results provide valuable references and enlightenment for this paper to study the effect of freezing of contact channels on the upper existing buildings [11,12].

In recent years, soil deformation caused by tunnel construction and its influence on underground structures has become a research focus. The free displacement field theory based on Gaussian distribution has been proposed, which lays a theoretical foundation for evaluating the influence of tunnel construction on underground pipelines [13,14]. On this basis, the continuous medium elastic solution of pipeline longitudinal deformation has been further derived, and the nonlinear change of soil stiffness has been considered, which makes the evaluation method more perfect [15,16]. Scholars have not only paid attention to the soil deformation caused by tunnel construction but also deeply studied the interaction mechanism between pipelines and soil. Considering the influence of soil stiffness weakening on pipeline bending stress, it has been found through model tests and numerical simulation that the longitudinal deformation of the pipeline can be more accurately predicted by considering the out-of-plane shear caused by pipe–soil interaction. In addition, there is more and more research on the discontinuous interface pipeline, and the calculation methods of pipeline deflection considering the interface effect have been proposed with respect to this, so that the simulation results are more close to the actual situation.

To simulate the deformation characteristics of the foundation more accurately, scholars have improved the foundation model. The traditional Winkler foundation model neglects the continuity of foundation deformation, while new models, such as the Pasternak foundation model, can better reflect the actual deformation of the foundation. Based on the Pasternak foundation model, the finite difference decomposition of discontinuous interface pipeline deflection has been constructed, which provides a new tool for evaluating the influence of freezing of the contact channel on superstructure. With the wide application of freezing technology in underground engineering, the changes of soil temperature field, seepage field, and stress field caused by freezing technology have been deeply studied by scholars at home and abroad. Remarkable achievements have been made in analytical solutions, the frost heave model, and experimental device development, which provide theoretical support for the application of freezing technology in the construction of subway connection passage. However, the research on the effect of freezing technology on the existing upper buildings is still insufficient, especially in the application of practical engineering validation, which needs to be strengthened. The improvement of the tunnel model itself has also been a research hotspot in recent years. The traditional tunnel model mainly simplifies the tunnel as an equal beam or Euler–Bernoulli infinite beam, but the urban shield tunnel is made of segments and bolts, and its physical and mechanical properties are weak. The Timoshenko beam model can better simulate the shear stiffness reduction effect of a tunnel, which provides a new idea for evaluating the influence of tunnel construction on underground structures. However, how to comprehensively consider the interaction between the tunnel, soil, and the superstructure in the concrete situation of freezing construction of the contact channel needs further research.

In summary, the study of tunnel–soil–building interaction has made some achievements, but there are still many deficiencies in the study of the influence of freezing of a contact passage on the existing upper structure. Through theoretical analysis, numerical simulation, and engineering measurement, this paper aims to deeply explore the changes in soil temperature field and stress field during the freezing process of a contact passage and its influence on the upper structure, to provide a scientific basis and technical support for the design and construction of underground engineering.

## 2. Project Overview

Dongge Road station–Binhu Road station is the 13th section of Nanning Rail Transit Line 3 from north to south, as shown in Figure 1. The depth of the tunnel is about 11.7~21.0 m. The starting point of this section is Dongge Road station, the end is Binhu Road station, the starting and ending mileage YDK14 + 778.298~YDK15 + 736.098, ZDK14 + 778.298~ZDK15 + 736.088, the short chain 4.485 m. The length of the left line is 953.306 m, and the length of the right line is 957.800 m. The interval tunnel is 6 m in diameter, and the line spacing is 4 m. The maximum slope of the line is 28.168%, and this section is a "V" shaped slope. The left line of this section adopts an earth pressure shield construction. The outer diameter D of the shield tunnel is φ6.0 m, and the thickness of the segment is 0.5 m. The construction (structure) in this section is mainly a water pipeline with a diameter of 3 m, and the concrete strength grade of the concrete pipeline is C40.


**Figure 1.** Location map of the shield tunnel in the Dongbin section.

The Dongbin section adopts the shield machine produced by Herrenkrenk, and the tunnel adopts the earth pressure shield tunneling. The tunnel in this section mainly passes through the boulder layer and soft plastic silty clay layer and partially passes through the silt layer and silty sand layer. The tunnel's buried depth is about 11.7 m.

## 3. The Establishment of a Numerical Model

### *3.1. Establishment of a Calculation Model of Freezing Body Temperature Field*

To facilitate the calculation, the following assumptions are made for the finite element model:

- The soil is continuous and homogeneous during freezing;
- When the soil is frozen, the latent heat of phase change is continuously released at the freezing interface;
- Assume that the moisture in the soil is completely frozen when it is cold; that is, the content of unfrozen water is zero [17,18];
- The freezing temperature load on the freezing hole wall of the model changes with the change in temperature;
- The wall of the freezing tube is negligible relative to the whole model, so the material characteristics of the freezing tube itself are not considered.

To analyze the influence of horizontal freezing of the contact channel on the existing tunnel in the upper part, according to the general situation of the project and the symmetry of the contact channel, this paper adopts the FLAC3D finite difference software to establish a structural model, and then realize the three-dimensional temperature field calculation of the frozen body. The position relationship between the frozen tube and the existing tunnel is shown in Figure 2. The total size of the model is 44 m long × 15 m wide × 35 m high, as shown in Figure 3.

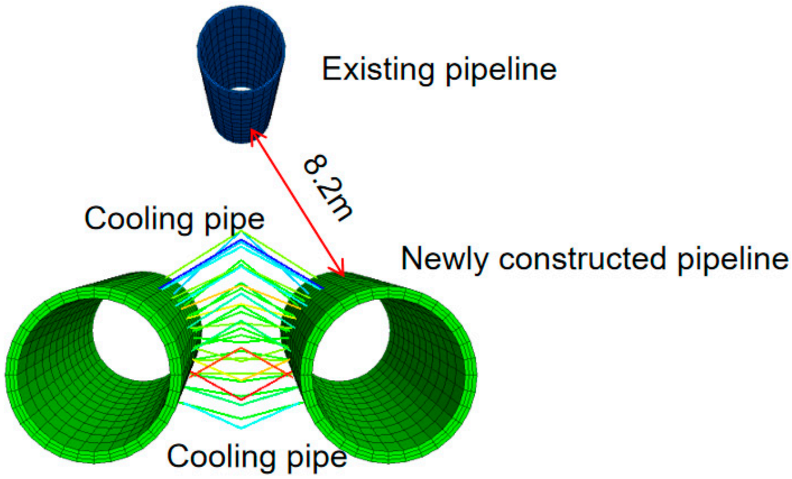


**Figure 2.** Position relationship between freezing tube and existing tunnel.

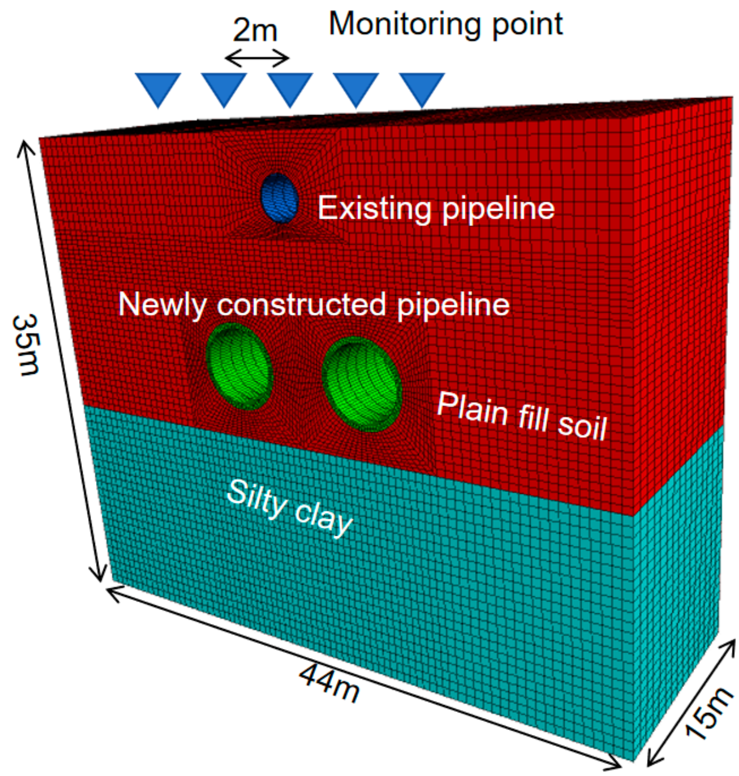


**Figure 3.** Numerical simulation grid model.

Application steps of FLAC3D in freezing method tunnel excavation calculation:

- According to the actual situation of the project, the three-dimensional geometric model, including tunnel, frozen soil wall, surrounding soil layer, and adjacent pipeline, is established in FLAC3D.
- Meshing ensures that the mesh density of the model is high enough at key locations, such as tunnel boundaries, the interface between the frozen wall, and the surrounding soil, to accurately capture stress concentration and deformation characteristics.
- The physical and mechanical parameters, such as elastic modulus, Poisson's ratio, density, cohesion and internal friction angle, are set according to laboratory tests or empirical formulas.
- Set the boundary conditions of the model, such as fixed boundaries, rolling boundaries, or free boundaries, to simulate the constraints in real situations.

- The freezing temperature field is set, the temperature gradient produced by the freezing tube in the soil is simulated, and the forming process of the frozen soil wall is calculated by a heat conduction equation.
- Monitoring the thickness, temperature distribution, and strength changes of the frozen soil wall, evaluating its supporting ability.
- According to the predetermined excavation sequence and excavation rate, the material of the tunnel is gradually removed to simulate the excavation process.
- In the process of excavation, the stress, strain, and displacement of soil around the tunnel are monitored in real time, especially the longitudinal deformation of adjacent pipelines.
- The simulation results are compared with the field-measured data to ensure the accuracy and reliability of the simulation results.
- The effects of different excavation rates, freezing temperatures, and other parameters on pipeline settlement are analyzed, and the conclusions mentioned in the abstract are verified.

When calculating the model numerically, the vertical tunnel axis direction in the water intake plane is the X axis, the direction along the tunnel axis is Y axis, and the vertical upward direction is the Z axis. In order to avoid the influence of a boundary effect on the numerical calculation results of the temperature field, the model range (X, Y, Z) was selected as (44, 15, 35 m), and considering the aspects of calculation accuracy and solution time, through the grid sensitivity analysis, we chose a set of grid configurations that can guarantee the calculation accuracy and control the calculation cost as the final simulation settings. The simulation results in this grid configuration are convergent and reliable enough to support our research conclusions.

The upper surface of the tunnel and frozen tube model is free, and the displacement of the lower surface and four side surfaces is completely constrained. The load is generated from top to bottom according to the gradient of gravity field considering only the action of gravity. The Mohr–Coulomb elastoplastic model was used as the soil element in the model. To make the calculation results more realistic, the model was subdivided into two layers, namely plain-filled soil and silty clay. The obtained rock and soil samples were brought back to the laboratory for various physical and mechanical tests, such as a density test, water content test, compression test, shear test, etc., in order to obtain the physical and mechanical parameters of rock and soil bodies, such as density, water content, compression modulus, internal friction angle, cohesion force, etc. The physical and mechanical parameters and thermophysical parameters of each soil layer are shown in Table 1. The elastic model was adopted for shield tunnel segment elements. The elastic modulus of the shield segment was set at 33.5 GPa, Poisson's ratio at 0.2, thermal conductivity at 0.5 W/(m °C), specific heat capacity at 1 kJ/(kg °C), and density at 2500 kg/m$^3$. Thermal conductivity of surface air and air in tunnel was 0.025 W/(m °C), and specific heat capacity was 1 kJ/(kg °C).

**Table 1.** Physical and mechanical parameters of rock and soil layer.

| Rock and Soil Stratification | Natural Density (g/cm$^3$) | Cohesion (kPa) | Angle of Friction (°) | Void Rating | Permeability Coefficient (m/d) | Coefficient of Lateral Pressure | Modulus of Elasticity (MPa) | Poisson's Ratio | Thermal Conductive (W/m/°C) | Specific Heat Capacity (J/kg/°C) |
|---|---|---|---|---|---|---|---|---|---|---|
| Plain fill soil | 1.96 | 15 | 10 | 0.752 | 3 | 0.35 | 4.5 | 0.35 | / | / |
| Silty clay | 1.98 | 38 | 13 | 0.710 | 0.006 | 0.33 | 6.5 | 0.33 | 1.85 | 1.46 |

In the actual freezing method construction process, the active freezing period of the interval contact channel is 40 d, and the numerical calculation time of the temperature field is also 40 d. Because the freezing pipe is arranged in an inclined radial shape, the freezing pipe layout on the upper and lower lines is not the same. It is a common and important step to arrange temperature measuring holes on site to monitor the temperature development of the freezing curtain during the construction of a freezing method of a subway contact passage. For the measurement of the temperature hole, there are usually repeated measurements to ensure the accuracy and reliability of the data. The instruments used to collect temperature data are usually high-precision temperature sensors or thermometers. These instruments can be installed in a temperature measuring hole and transmit temperature data wired or wirelessly to a data acquisition system or monitoring center. The temperature sensors in the temperature measurement holes must be installed and arranged according to the design requirements. At the same time, in order to ensure the accuracy of the measurement data, the front end of the temperature measurement tube should be welded and sealed, and no water should be permeated in the tube.

For the convenience of analysis, a typical cross-section in the direction of Y = −7.5 was selected, respectively, and a total of five temperature measuring holes were arranged, as shown in Figure 3. The data of the same point in the temperature measuring holes C1 and C3 in the tunnel were, respectively, taken as representatives, and the temperature change value was recorded according to the actual temperature measuring point in the numerical simulation. After 40 days of active freezing, the comparison between the numerical simulation of the temperature curves of the two temperature measuring holes and the field-measured temperature is shown in Figure 4.

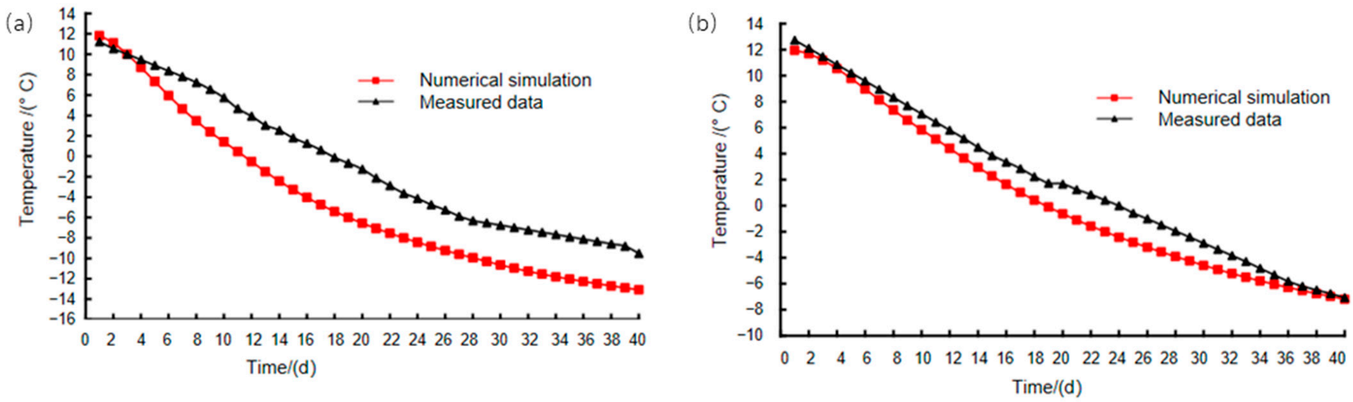


**Figure 4.** Comparison of temperature curves: (**a**) C1, (**b**) C3.

As shown in Figure 4, the average cooling velocity of the C1 temperature measuring hole is about 0.54 °C/d, and the numerical result is about 0.63 °C/d. After 40 days of active freezing, the measured temperature of the C1 temperature measuring hole is −9.50 °C, and the numerical simulation temperature is −13.10 °C. As shown in Figure 4, the average cooling speed of the C10 temperature measuring hole is about 0.48 °C/d, and the numerical result is about 0.48 °C/d. After active freezing for 40 days, the measured temperature of the C10 temperature measuring hole is −7.06 °C, and the numerical simulation temperature is −7.18 °C. It can be seen that the temperature cooling trends of the numerical simulation results at the same temperature measuring points are the same as that of the field-measured results. On the whole, the numerical simulation results are slightly lower than the measured temperature value, because the numerical calculation assumes that the groundwater is static. In the actual project, because the groundwater is flowing, the heat exchange of the frozen soil curtain is more complicated, and the flow of the groundwater will take away part of the cold amount, so the numerical simulation result is slightly lower than the measured temperature value. In summary, it can be shown that the transient freezing temperature field obtained by the numerical simulation of the finite difference method software FLAC 3D can reflect the actual situation of the project.

### *3.2. Pipeline Stress and Deformation Law during the Excavation of Contact Passage*

After the excavation of the left and right sides of the tunnel, the change law of pipe stress and displacement is shown in Figures 5 and 6. It can be seen from Figures 5 and 6 that the breaking of the segment will lead to the redistribution of the stress field and displacement field in a certain surrounding area. Compared with the intact segment on the right, local stress concentration will occur after the segment is broken. As shown in Figure 5, the maximum stress value reaches 12.5 MPa, which is mainly concentrated in the bottom corner and the center area of the bottom edge of the segment opening. For shield tunnel segments using concrete with C50 strength grade, the safety factor is 4, the pipeline stress is only 0.78 MPa, and the safety factor is 50, which is within the safe range. At the same time, the breaking of the segment will cause the frozen soil curtain near the opening to shift into the tunnel, as shown in Figure 5. The displacement is very small, and the maximum displacement value is less than 10 mm. Whether in terms of stress or displacement, the breaking of the segment is within the safe range, and the construction can be carried out normally.

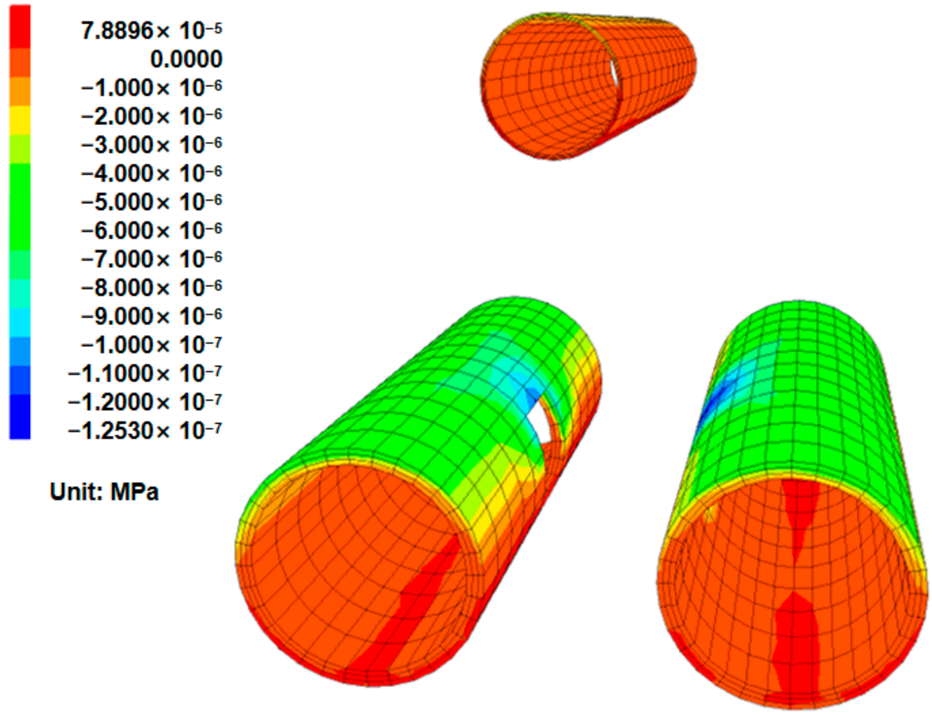


**Figure 5.** Stress program after fragment breaking.

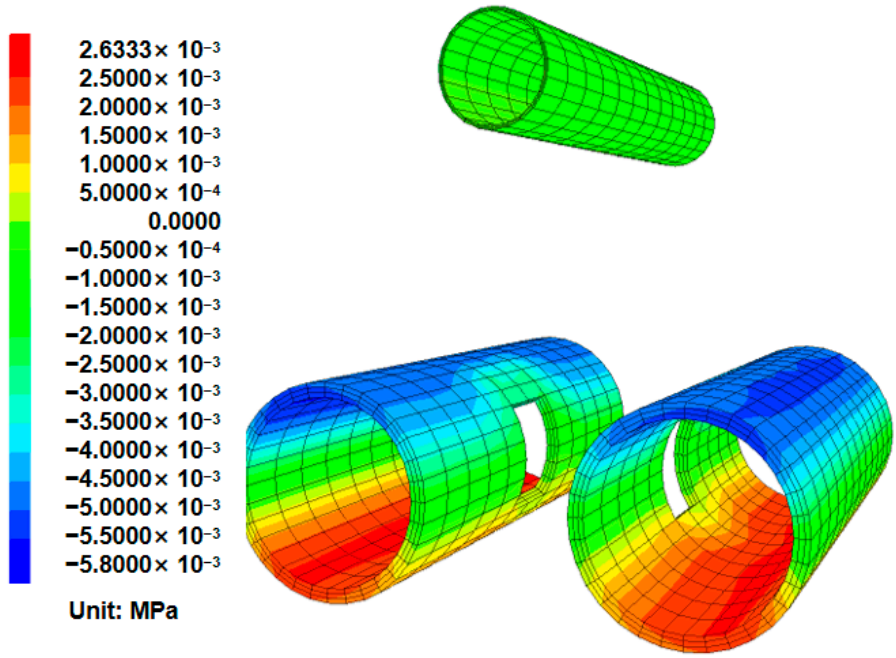


**Figure 6.** Displacement equivalent cloud map after segment break.

After the tunnel excavation, the deformation diagram of the tunnel and pipeline is shown in Figure 7. Without the initial support, the maximum subsidence value of the vault displacement is 11.8 mm, the maximum uplift value of the floor displacement is 13.2 mm, and the pipeline displacement is 10 mm, which is within the safe range.

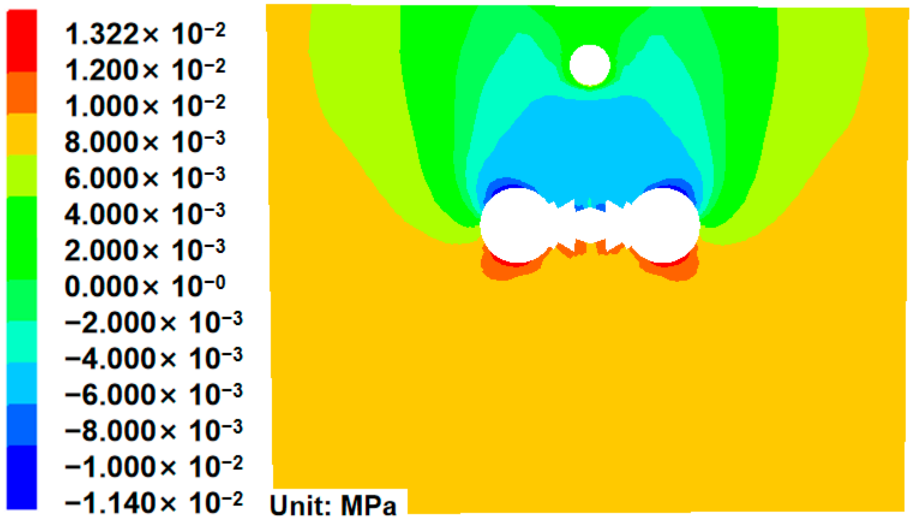


**Figure 7.** Z-displacement cloud image of the model after tunnel excavation.

## 4. Theoretical Derivation

### *4.1. Mechanical Model and Basic Assumptions*

Figure 7 shows the engineering problem to be solved. The formation loss caused by the excavation of the circular shield tunnel causes the overlying strata to displace and then causes the underground pipeline to bend. As shown in Figure 8, the $x$ coordinate is used to mark the position of each section along the pipeline. The theoretical derivation of this paper is based on the following basic assumptions and simplifications: tunnels and pipelines are buried horizontally in homogeneous isotropic strata, and their axes are perpendicular to each other. The foundation around the pipeline is simplified to the Pasternak foundation.

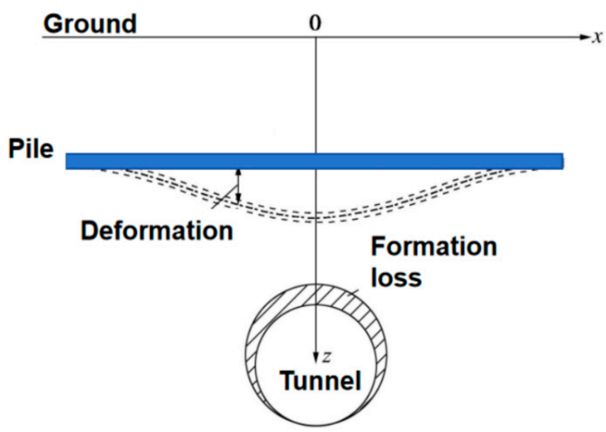


**Figure 8.** Schematic diagram of pipeline deflection caused by shield tunnel excavation.

### *4.2. Construction of Pipeline Deflection Differential Equation*

As shown in Figure 9, the left and right ends of any joint position are intercepted with dx length for force analysis. It is assumed that they act on the line axis position and are evenly distributed along the y *direction*.

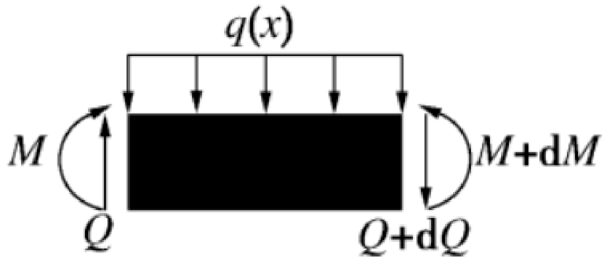


**Figure 9.** Element force analysis: micro force analysis of the left end of the joint.

Firstly, the vertical force balance of the microelement can be obtained using

$$(Q - \mathrm{d}Q) - q(x)b\mathrm{d}x - Q = 0 \tag{1}$$

where dx is the element width (m), q is the cross-section shear force (N), is the increment of cross-section shear force (N) along the length of dx of the pipeline, q(x) is the foundation reaction force *acting* on the pipeline ($N/m^2$), and b is the diameter of the pipeline (m).

Equation (1) can be obtained by simplification

$$\frac{\mathrm{d}Q}{\mathrm{d}x} = -q(x)b \tag{2}$$

Secondly, find the bending moment of the section of the left end of the element, which can be obtained by balancing the bending moment

$$(M - \mathrm{d}M) + Q\mathrm{d}x + q(x)b\frac{(\mathrm{d}x)^2}{2} - M = 0 \tag{3}$$

where $M$ is the cross-section bending moment (N·m), and dM is the increment of the cross-section bending moment (N·m) along the dx length of the pipeline.

Equation (3) simplifies and omits the second-order trace, which can be obtained by

$$\frac{\mathrm{d}M}{\mathrm{d}x} = Q \tag{4}$$

Equation (2) is obtained in conjunction with (4):

$$q(x) = -\frac{1}{b}\frac{\mathrm{d}^2M}{\mathrm{d}x^2} \tag{5}$$

Suppose the force of the pipeline on the surrounding formation is $p(x)$, and its interaction with $q(x)$ is the interaction force, then

$$p(x) = -q(x) \tag{6}$$

Assuming that the bending stiffness of any cross-section of the pipeline along the direction is infinite, the pipeline will produce an overall translation along the $y$ direction when it interacts with the soil. Combined with the assumption that the pipeline is always in contact with the surrounding strata, the vertical displacement u($x$) of the soil on the contact surface of any cross-section of the pipeline will not change along the direction. Therefore, when the pipeline interacts with the soil, the relationship between the pipeline force $p(x)$ and the ground displacement u(x) caused by the pipeline can be expressed as Equation (7).

$$p(x) = ku(x) - G_\mathrm{p}\frac{\mathrm{d}^2u(x)}{\mathrm{d}x^2} \tag{7}$$

where $k$ is the foundation reaction coefficient ($N/m^3$) and $Gp$ is the foundation shear stiffness (N/m).

Simultaneous Equation as (5)–(7) can be obtained

$$\frac{\mathrm{d}^2 M}{\mathrm{d}x^2} = kbu(x) - G_\mathrm{p} b \frac{\mathrm{d}^2 u(x)}{\mathrm{d}x^2} \tag{8}$$

Similarly, for the right end of the joint and the standard pipe section, Equation (8) can be deduced.

The formation displacement around the pipeline originates from two aspects, one is the formation settlements ($x$) caused by the formation loss in tunnel excavation, and the other is the foundation displacement u(x) caused by the interaction between the pipeline and the soil. Assuming that the axial deflection along the pipeline is $w(x)$, the Equation (9) can be obtained based on the assumption that the pipeline is always in contact with the surrounding strata.

$$w(x) = s(x) + u(x) \tag{9}$$

In the Equation, $s(x)$ and $u(x)$ are taken from the position of the pipeline axis. By combining Equation as (8) and (9), we can obtain

$$-\frac{\mathrm{d}^2 M}{\mathrm{d}x^2} + kbw(x) - G_\mathrm{p} b \frac{\mathrm{d}^2 w(x)}{\mathrm{d}x^2} = kbs(x) - G_\mathrm{p} b \frac{\mathrm{d}^2 s(x)}{\mathrm{d}x^2} \tag{10}$$

The deflection w(x) satisfies the Equation (11) of the extramural differential equation.

$$\frac{\mathrm{d}^2 w(x)}{\mathrm{d}x^2} = -\frac{M}{EI} \tag{11}$$

where E is the elastic modulus ($\mathrm{N/m^2}$) of the pipeline and I is the moment of inertia of the pipeline cross-section. By substituting Equation (11) into Equation (10), we can obtain

$$-\frac{\mathrm{d}^2 M}{\mathrm{d}x^2} + kbw(x) + G_\mathrm{p} b \frac{M}{EI} = kbs(x) - G_\mathrm{p} b \frac{\mathrm{d}^2 s(x)}{\mathrm{d}x^2} \tag{12}$$

The cross-sectional ground settlement s(x) perpendicular to the tunnel axis caused by ground loss in tunnel excavation conforms to the distribution pattern of the Gaussian curve, namely Equation (13).

$$s(x) = \frac{\pi R^2 V_1}{\sqrt{2\pi} K (z_0 - z_\mathrm{p})} \exp\left[-\frac{x^2}{2K^2 (z_0 - z_\mathrm{p})^2}\right] \tag{13}$$

where $R$ is the outer radius of the tunnel (m), $Vl$ is the ground layer loss caused by tunnel excavation (dimension is 1), $K$ is the width parameter of the settlement tank at the position of the pipeline axis (dimension is 1), and $z0$ and $zp$ are divided into the axis burial depths of the tunnel and pipeline (m).

$$\frac{\mathrm{d}^2 M}{\mathrm{d}x^2} = -EI \frac{\mathrm{d}^4 w(x)}{\mathrm{d}x^4} \tag{14}$$

Substitute Equation (14) into Equation (10) to obtain

$$\begin{aligned} EI \frac{\mathrm{d}^4 w(x)}{\mathrm{d}x^4} + kbw(x) - G_\mathrm{p} b \frac{\mathrm{d}^2 w(x)}{\mathrm{d}x^2} \\ = kbs(x) - G_\mathrm{p} b \frac{\mathrm{d}^2 s(x)}{\mathrm{d}x^2} \end{aligned} \tag{15}$$

The calculation Equations of foundation shear stiffness $Gp$ are as follows: Equations (16) and (17).

$$G_\mathrm{p} = \frac{E_\mathrm{s} H_\mathrm{t}}{6(1 + v_\mathrm{s})} \psi_\mathrm{t} \tag{16}$$

$$\psi_t = \frac{3}{2\gamma_p H_t}\frac{\sinh(\gamma_p H_t)\cosh(\gamma_p H_t) - \gamma_p H_t}{\sinh^2(\gamma_p H_t)} \tag{17}$$

where *Es* is the elastic modulus of the soil mass (N/m$^2$), vs. is the Poisson ratio of the soil mass, Ht is the thickness of the foundation shear layer (m), and Yp is the empirical *parameter* (M-1).

The algebraic equations applicable to each difference node are integrated into the following matrix form:

$$[K_p]\{w\} + [K_r]\{w\} - [K_{s1}]\{w\} = [K_r]\{s\} - [K_{s2}]\{s\} \tag{18}$$

where [*Kp*] is the stiffness matrix of the pipeline, [*Kr*] is the foundation reaction stiffness matrix, [*Ks1*] and [Ks2] are two different foundation shear stiffness matrices, {w} is the *pipeline* flexure vector, and {s} is the formation settlement vector generated by formation loss in tunnel excavation at each difference junction point.

Each matrix and vector can be obtained by Equation (18) and determined by the algebraic equations of the above-mentioned difference nodes.

### 4.3. Verification of the Theoretical Model

In order to verify the accuracy of the theoretical model, the calculation results of the theoretical model were compared with the Equation calculation results in Yao, Y. et al., (2023) [16], field monitoring data, and simulation data generated by the numerical model, as shown in Figure 10. The comparison results are shown in Figure 10. It can be seen from Figure 10 that the simulation results are highly consistent with the measured data, which proves the feasibility of the numerical simulation method. However, due to the limitation of simplified conditions, the influence of the Timoshenko beam theory on the longitudinal deformation of the pipeline is not fully reflected in the numerical simulation, resulting in a small width of the predicted settlement curve.

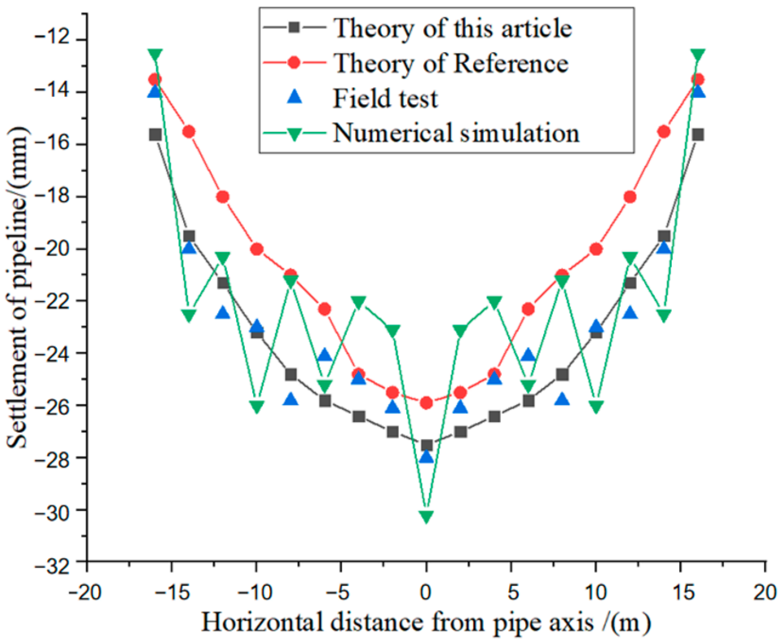


**Figure 10.** Comparison of a theoretical model with numerical simulation and measured data [16].

### 4.4. Influence of Tunnel Excavation Rate on Pipeline Settlement

Statistics on the influence of tunnel excavation rate on pipeline settlement are shown in Figure 11. The influence of daily tunnel excavation length (DEL) on pipeline settlement is analyzed. As can be seen from Figure 11, the faster the excavation rate of the tunnel, the greater the disturbance to the surrounding soil mass, which may lead to rapid changes in the formation stress and strain state, and then lead to more significant surface deformation. This deformation has an adverse effect on underground pipelines. When the excavation rate is less than 1.0 m per day, the settlement of the pipeline is less than 30 mm, while when the excavation rate is greater than 1.0 m per day, the settlement of the pipeline increases rapidly. Therefore, in the tunnel design and construction stage, it is necessary to comprehensively consider the geological conditions, excavation methods, and supporting measures, and reasonably control the excavation rate to reduce the impact on surface deformation to ensure construction safety and stability of the surrounding environment.

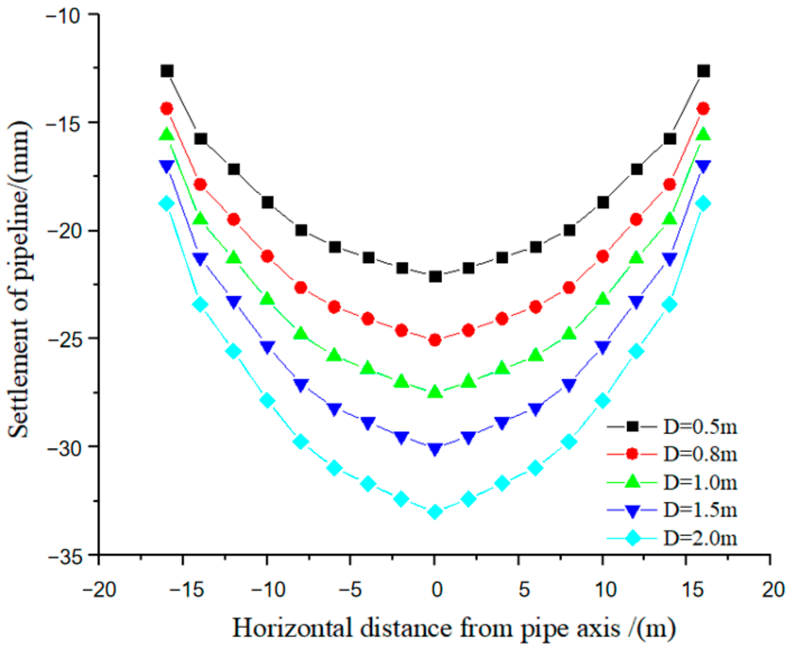


**Figure 11.** Influence of tunnel excavation rate on pipeline settlement.

### *4.5. Influence of Tunnel Freezing Temperature on Pipeline Settlement*

The statistical relationship between tunnel freezing temperature and pipeline settlement shown in detail in Figure 12 deeply reveals the key role of temperature factor in the stability control of tunnel construction. Specifically, when a lower freezing temperature (such as −50 °C) is used, this extremely low-temperature environment significantly promotes the formation of frozen soil walls or frozen soil bodies, which not only increase in thickness, but also significantly improve in strength. This strengthening effect greatly enhances the support ability of the frozen soil structure to the surrounding soil, which is like building a solid barrier, effectively limiting the range and degree of formation disturbance during tunnel excavation, thereby reducing the formation settlement caused by construction activities.

On the other hand, the phenomenon of frost heave induced by low temperature is particularly significant in the soil above the tunnel, showing obvious uplift phenomenon. Although this uplift may seem unfavorable at the early stage of freezing, because it changes the original formation shape, it actually provides a “pre-compression” effect for the subsequent excavation process. However, with the gradual excavation of the tunnel, the soil uplifted by frost heave quickly loses its support and is transformed into a significant settlement. It is worth noting that this settlement often has a large magnitude and a certain lag; that is, the initial settlement may not be obvious, but with the passage of time and stress redistribution, the settlement will gradually increase.

Specific to the numerical value, comparing the pipe settlement under the two freezing conditions of −50 °C and −15 °C, we can clearly see the significant impact of temperature difference. At a low temperature of −50 °C, thanks to the stronger frozen soil support effect, the settlement of the pipeline is effectively controlled above −20 mm, showing a better construction control effect. In contrast, when the freezing temperature is increased to −15 °C, the strength and thickness of the frozen soil wall or frozen soil body are weakened, and the supporting effect on the surrounding soil is reduced, resulting in a significant increase in pipeline settlement to −33.2 mm, highlighting the important role of low-temperature freezing in controlling the settlement of tunnel construction.

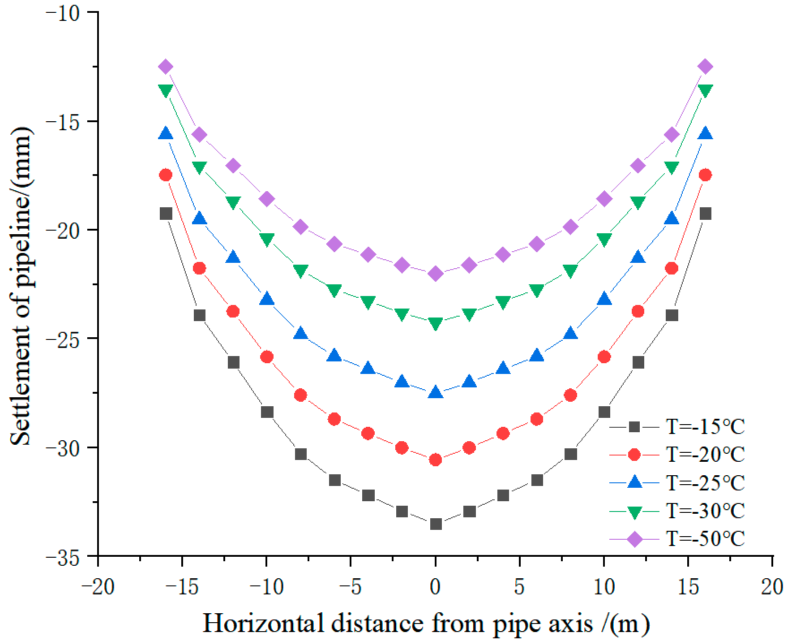


**Figure 12.** Influence of tunnel freezing temperature on pipeline settlement.

### *4.6. Influence of Thickness of the Frozen Curtain on Pipeline Settlement*

To delve deeper into the complex relationship between the thickness of the frozen curtain and pipe settlement presented in Figure 13, we can explore the underlying physical mechanisms and engineering effects. With the increase in the thickness of the frozen curtain, its performance as a support structure is significantly enhanced, which is comprehensive in nature. Firstly, the thicker frozen curtain acts as a more solid barrier, and its enhanced support capacity is directly reflected in the effective resistance to the surrounding soil pressure and deformation. This enhanced resistance not only limits the scope and intensity of soil disturbance during tunnel excavation, but also significantly reduces the resulting soil settlement, providing important assurances for the safety and stability of tunnel construction.

During another critical stage of tunnel construction—the thawing process—the thicker frozen curtains also exhibit their unique advantages. With higher strength and stability, these thick frozen soil walls can release internal stress more slowly and contentedly in response to the challenge of melting, thus reducing the risk of sudden subsidence caused by rapid melting. Smaller melting volume and slower melting speed mean that the stability of the subsurface structure is better maintained, which is conducive to the smooth progress of construction and the improvement of final engineering quality.

It is particularly noteworthy that when the thickness of the frozen curtain is increased from 0.5 m to 1 m, the subsidence phenomenon above the tunnel shows a significant reduction. This transition indicates that the 1 m thick frozen curtain has been able to exert a strong support role during excavation, effectively alleviating the negative impact of ground disturbance. However, as the thickness of the frozen curtain is further increased to 2 m, although the subsidence volume continues to decrease, the rate of decrease is not as significant as before. This phenomenon can be explained from the perspective of mechanics and the saturation effect of materials: when the frozen curtain reaches a certain thickness, the growth of its bearing capacity will gradually become flat, i.e., reaching a “saturated” state. At this point, the marginal benefits of further increasing the thickness for subsidence control will gradually decrease.

In summary, the rational design of tunnel freezing curtain thickness is one of the key factors in controlling pipe settlement, ensuring construction safety and engineering quality. By scientific calculation and engineering practice, determining the optimal freezing curtain thickness can effectively reduce ground disturbance and settlement while optimizing construction costs and time, achieving a win–win situation of economic benefits and social benefits.

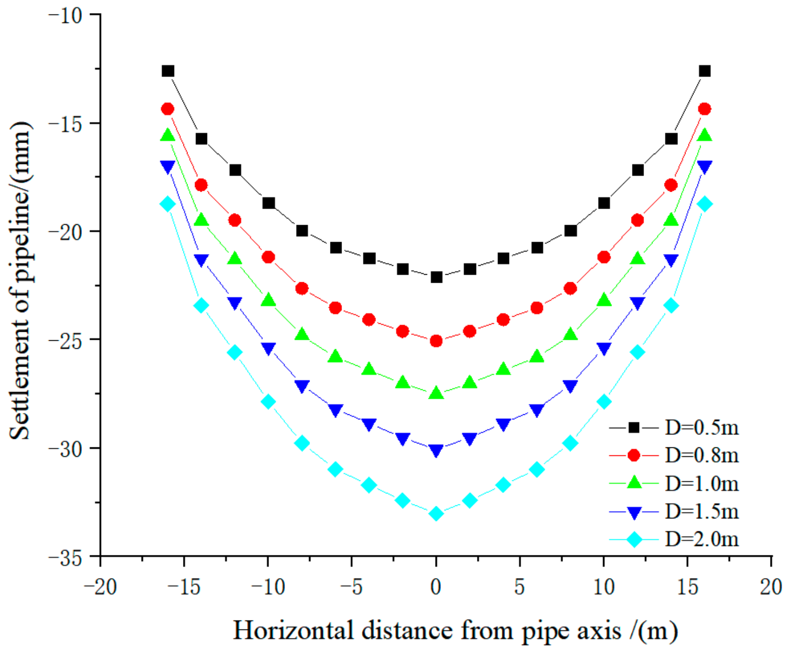


**Figure 13.** Influence of tunnel freezing temperature on pipeline settlement.

### *4.7. Safety Assessment of Buried HDPE Bellows Affected by Excavation*

The pipe used in this paper is the HDPE corrugated pipe for water supply. According to the above results, the maximum circumferential allowable strain of the pipe can be determined according to article 4.4.6 in reference [19]; that is, the maximum vertical deformation of the polyethylene pipe under the combined action should be calculated as follows:

$$\omega_{d,max} \leq 0.05D_0 \tag{19}$$

where $\omega_{d,max}$ is the maximum vertical deformation of the polyethylene pipeline under the combined action, and D0 is the calculated diameter of the pipeline. The maximum allowable compressive and tensile strains are 5%.

According to the full text analysis, under different working conditions, the maximum settlement of the pipeline is less than 55 mm, while the allowable deformation of the pipeline is 150 mm. Therefore, the research in this paper can provide a basis for the excavation of refrigerated contact channels, and it can provide ideas for the safety criteria of pipelines.

## 5. Conclusions

- The breaking of the segment will lead to the redistribution of the stress field and displacement field in a certain surrounding area. Compared with the complete segment, the phenomenon of local stress concentration will occur after the segment is broken. Whether in terms of stress or displacement, the broken segment is within the safe range, and the construction can be carried out normally.
- The prediction theory of stratum displacement caused by tunnel excavation has an important impact on the estimation of pipeline longitudinal deformation. The tunnel

longitudinal deformation trend obtained based on the Euler–Bernoulli beam longitudinal prediction theory is consistent with the measured results.

- The faster the tunnel excavation speed, the greater the disturbance to the surrounding soil. When the excavation rate is less than 1.0 m/d, the pipeline settlement is less than 30 mm, and when the excavation rate is greater than 1.0 m/d, the pipeline settlement increases rapidly. The lower the freezing temperature, the thicker and stronger the frozen soil wall or frozen soil body, and the stronger the supporting effect on the surrounding soil. With the increase of freezing curtain thickness, the supporting ability of the freezing curtain is obviously enhanced. Thicker freezing curtains can resist the pressure and deformation of surrounding soil more effectively, thus reducing the formation disturbance and settlement caused by tunnel excavation.
- This paper mainly considers the influence of tunnel excavation on the existing pipeline when the formation is relatively uniform, and also provides readers with a way to judge the safety of the pipeline. If the stratification between new and old tunnels is obvious, the stratification effect should be further considered. In general, the analytical solution of pipe settlement caused by tunnel excavation presented in this paper can provide theoretical support for analyzing the influence of tunnel excavation on existing pipes.

**Author Contributions:** Conceptualization, J.Z., J.L., S.F. and Z.H.; methodology, S.F.; software, J.Z.; validation, J.Z.; writing—original draft preparation, S.F. and J.L.; writing—review and editing, J.L. and J.Z.; project administration, Z.H. and J.Z.; funding acquisition, J.Z. and J.L. All authors have read and agreed to the published version of the manuscript.

**Funding:** This research was supported by National Natural Science Foundation of China (NO. 52108386). The authors are deeply indebted to the financial support.

**Data Availability Statement:** Data is contained within the article.

**Conflicts of Interest:** Author J.Z. was employed by the company CCCC Second Highway Consultant Co., Ltd. The author declares no conflict of interest.

## References

1. Li, Y.; Yao, A.; Gao, X.; Li, H.; Gong, Y. Rapid Prediction of Pile Friction Resistance Based on Soil Deformation Law Caused by a Super Large Diameter Tunnel: A Case Study. *KSCE J. Civ. Eng.* **2024**, *28*, 3033–3041. [CrossRef]
2. Zhang, J.; Pan, T.; Ma, K.; Xu, Q.; Kong, C. Modified stochastic medium prediction model for the deformation response of concealed underground stations under existing pipelines. *Sci. Rep.* **2023**, *13*, 9843. [CrossRef] [PubMed]
3. Li, Y.; Huang, C.; Lu, H.; Mou, C. Deformation Prediction Model of Existing Tunnel Structures with Equivalent Layered Method–Peck Coupled under Multiple Factors. *Mathematics* **2024**, *12*, 1479. [CrossRef]
4. Yamada, Y. A theoretical prediction method of inclined crack width in evaluation model for capacities of shear resistance mechanisms of RC beams. *J. Jpn. Soc. Civ. Eng. Ser. E2 (Mater. Concr. Struct.)* **2022**, *78*, 264–273. [CrossRef] [PubMed]
5. Guo, J. An Evaluation Model of the Stuck Risks Based on Remote Sensor Network and Fuzzy Logic. *IEEE Sens. J.* **2021**, *21*, 23658–23666. [CrossRef]
6. Wang, L.; He, C.; Cui, S.; Wang, F. Numerical Simulation of Surface Movement and Deformation Caused by Underground Mining with Complex Stratigraphic Boundary. *Adv. Civ. Eng.* **2021**, *2021*, 9967071. [CrossRef]
7. Huang, J.; Liu, J.; Guo, K.; Yang, S.; Lu, Y.; Wang, Y.; Wu, C. Evaluation Method of the Impact of Twin Shield Tunneling Construction on Elevated Bridges: Case Study. *Symmetry* **2024**, *16*, 1113. [CrossRef]
8. Liu, Q.; Shao, B.; Wang, B.; Zhang, W.; Ju, Z.; Ma, X.; Wang, P. Research on Prediction and Prevention of Nonuniform Deformation in Unsymmetrical Loading Tunnel. In Proceedings of the Engineering Geology for a Habitable Earth: IAEG XIV Congress 2023, Chengdu, China, 21–27 September 2023; Springer: Singapore, 2024. [CrossRef]
9. Li, F.; Tang, Q.; Yan, W.; Li, J.; Li, W.; Yang, T.; Lin, L.; Jiang, K.; Wang, K.; Zhang, W. Research on the failure analysis and prediction method of casing deformation under the synergistic effect of sand production and corrosion. *Eng. Fail. Anal.* **2023**, *154*, 107706. [CrossRef]
10. Ma, J.; Huang, K.; Zou, B.; Li, X.; Deng, Y. The influence of tunnel insulation measures on the temperature spatiotemporal variation of frozen soil during artificial ground freezing. *Cold Reg. Sci. Technol.* **2023**, *214*, 103942. [CrossRef]
11. Xu, X.; Wu, Z.; Weng, L.; Chu, Z.; Liu, Q.; Zhou, Y. Numerical investigation of geostress influence on the grouting reinforcement effectiveness of tunnel surrounding rock mass in fault fracture zones. *J. Rock Mech. Geotech. Eng.* **2024**, *16*, 81–101. [CrossRef]
12. Wu, X.; Gong, M.; Wu, G.W.S. Vibration reduction technology and the mechanisms of surrounding rock damage from blasting in neighborhood tunnels with small clearance. *Int. J. Min. Sci. Technol.* **2023**, *33*, 625–637. [CrossRef]

13. Qin, Z.; Liu, Y.; Liu, J.; Cao, B.; Zhang, F.; Li, W. Application of pretensioned grouting support in repairing surrounding rock damaged by dynamic load. *Arab. J. Geosci.* **2022**, *15*, 922. [CrossRef]
14. Zhang, S.; Lai, Y.; Zhang, X.; Pu, Y.; Yu, W. Study on the damage propagation of surrounding rock from a cold-region tunnel under freeze–thaw cycle condition. *Tunn. Undergr. Space Technol.* **2004**, *19*, 295–302. [CrossRef]
15. Zhang, X.; Lai, Y.; Yu, W.; Zhang, S. Non-linear analysis for the freezing–thawing situation of the rock surrounding the tunnel in cold regions under the conditions of different construction seasons, initial temperatures and insulations. *Tunn. Undergr. Space Technol.* **2002**, *17*, 315–325. [CrossRef]
16. Yao, Y.; Zhu, Y.; Shen, D.; Zhang, Z.; Wang, W. Fuzzy random evaluation of creep model of frozen soft soil in metro tunnel construction using artificial ground freezing technique. *Sci. Rep.* **2023**, *13*, 9468. [CrossRef] [PubMed]
17. Chen, J.H.; Zhang, J.; Chen, B.J.; Lu, G. The influence of the underpassing frozen connecting passage on the deformation of the existing tunnel. *Res. Cold Arid. Reg.* **2022**, *14*, 258–266. [CrossRef]
18. Chen, B. *Study on Mechanism of Freezing of Contact Channel on Existing Upper Tunnel*; Fujian College of Engineering: Fujian, China, 2021. (In Chinese)
19. *DBJ52/T039-2017*; Technical Regulations for Outdoor Buried Polyethylene (PE) Water Supply Pipeline Engineering. Guizhou Provincial Department of Housing and Urban-Rural Development: Guizhou, China, 2018.